

Investigation of the DEMO WCLL Breeding Blanket Cooling Water Activation

P. Chiovaro^{a*}, S. Ciattaglia^b, F. Cismondi^b, A. Del Nevo^c, P.A. Di Maio^a, G. Federici^b, C. Frittitta^a, I. Moscato^a, G. A. Spagnuolo^d, E. Vallone^a

^aDipartimento Ingegneria, Università di Palermo, Viale delle Scienze, 90128, Palermo, Italy

^bEUROfusion Consortium, Boltzmannstr.2, Garching, 85748, Germany

^cENEA Brasimone I, Camugnano, BO 40032, Italy

^dKarlsruhe Institute for Technology (KIT), Hermann-von-Helmholtz-Platz 1, 76344 Eggenstein-Leopoldshafen, Germany

*Corresponding author: pierluigi.chiovaro@unipa.it

Within the framework of the activities foreseen by the EUROfusion action on the cooling water activation assessment for a DEMO reactor equipped with a Water Cooled Lithium Lead Breeding Blanket (WCLL BB), the University of Palermo is involved in the assessment of dose rates induced by the decay of nitrogen radioisotopes produced by water activation, nearby the main components (e.g. isolation valves) of both First Wall (FW) and Breeder Zone (BZ) cooling circuits. In particular, the aim of this work is to evaluate the spatial distribution of nitrogen isotopes (^{16}N and ^{17}N) in the WCLL BB cooling circuits. To this purpose, a coupled neutronic/fluid-dynamic problem is solved following a theoretical-numerical approach and adopting an integrated computational tool mainly relying on the use of MCNP6 and ANSYS CFX codes. The operative procedure adopted foresees the assessment of the production rate distributions of nitrogen isotopes within FW and BZ cooling channels and tubes by means of totally heterogeneous neutronic analyses. A fully 3-D fluid-dynamic approach is, then, used to compute the nitrogen isotope concentrations within the In-Vessel complex flow domain, while a 1-D lumped parameters approach is adopted to calculate their distribution along the Ex-Vessel BB Primary Heat Transfer System. The results obtained, herewith presented and critically discussed, provided the necessary data to perform dedicated neutronic and photonic transport analyses and, hence, to assess the dose rates in the aforementioned target locations.

Keywords: DEMO reactor; WCLL Blanket; neutronics; fluid-dynamics.

1. Introduction

Within the framework of the activities foreseen by EUROfusion action (TS Ref. PMI-3-T011) on the “Cooling water activation assessment”, the University of Palermo is involved in the dose assessment around both First Wall (FW) and Breeder Zone (BZ) cooling circuits (e.g. isolation valves, hot and cold legs) of the DEMO reactor equipped with a Water Cooled Lithium Lead Breeding Blanket (WCLL BB) [1]. In such a nuclear system the endothermic charged-particle reactions $^{16}\text{O}(n,p)^{16}\text{N}$ (with a threshold energy of ~ 10.2 MeV) and $^{17}\text{O}(n,p)^{17}\text{N}$ (with a threshold energy of ~ 8.4 MeV) are the principal sources of water radioactivity during operation [2,3]. ^{16}N decays by emission of β particle and emits γ rays with an half-life of 7.13 s while ^{17}N decays by β particles and emits neutrons with an half-life of 4.173 s. The aim of this research activity is to assess the spatial distribution of the absorbed dose, due to the decay of nitrogen isotopes produced by coolant activation, around some key components of WCLL BB cooling circuit and nearby their locations **in order to evaluate it on valve electronic actuators and hydraulic seals (if made of organic materials) and eventually – to study some dose mitigation actions. As far as this paper is concerned, it aims at assessing** the spatial distribution of nitrogen isotope concentrations in the WCLL BB cooling circuits, focussing the attention on the Primary

Heat Transfer System (PHTS). **The map of nitrogen isotope concentrations, herewith shown, then, have been used to set up the photon and neutron sources for the dose spatial distribution assessment presented in a further work [4].** Therefore, a coupled neutronic/fluid-dynamic problem has been solved following a theoretical-numerical approach and adopting an integrated computational tool mainly relying on the use of MCNP6 and ANSYS CFX codes. Neutronic calculations to evaluate the spatial distribution of the production rates of nitrogen isotope concentrations have been performed following a computational approach based on the Monte Carlo method and adopting the Monte Carlo N-Particle (MCNP6.2) code [5] along with the JEFF-3.2 transport cross section libraries [6]. With regard to the 3D computational fluid-dynamic analyses (CFD), the Finite Volume Method has been used, adopting the ANSYS CFX 19.2 code [7] to assess the nitrogen isotope concentrations. In particular, MCNP6 capability to perform calculations on hybrid geometries that consist of ABAQUS code Unstructured Mesh (UM) geometry representations embedded as universes in its legacy constructive solid geometry [8] and the ANSYS Finite Element Modeler capability of exporting mesh files in a ABAQUS like format have been exploited to couple the aforementioned problems. As far as the WCLL BB and its PHTS are concerned, attention has been focused on 2018 design [9-11], which foresees the

blanket to be arranged in a Single Module Segment layout adopting two parallel and distinct cooling circuits for FW and BZ.

2. Description of the method

The leading physical quantity of this research activity is the spatial distribution of the absorbed dose in some target locations. In order to assess such a quantity it is necessary to compute the spatial distribution of the activity volumetric density: $\lambda n(x_i, t)$, where λ is the decay constant of the given isotope and $n(x_i, t)$ is the spatial distribution of its concentration. Indeed, the knowledge of the volumetric density of the activity spatial distribution allows the set-up of photon (^{16}N) and neutron (^{17}N) sources for the dose calculations by means of nuclear analyses. In turn, the activity depends by isotope concentrations, so, in order to determine the spatial distribution of the nitrogen isotope volumetric densities, a fluid-dynamic problem must be solved taking into account both the conservation equations for the flow and the passive scalar transport equations for the nitrogen isotopes, with the opportune boundary conditions:

$$\begin{cases} \frac{\partial(\rho u_i)}{\partial x_i} = 0 \\ \rho u_j \frac{\partial u_i}{\partial x_j} = -\frac{\partial p}{\partial x_i} + \frac{\partial}{\partial x_j} \left[\mu \left(\frac{\partial u_i}{\partial x_j} + \frac{\partial u_j}{\partial x_i} \right) \right] + f_{i,v} \\ u_i \frac{\partial n_N}{\partial x_i} - \Gamma \frac{\partial^2 n_N}{\partial x_i^2} = R^N - \lambda_N n_N \end{cases}$$

where: ρ is the water density, u_i are its velocity components, p is the pressure, μ is the viscosity, $f_{i,v}$ are the volume density forces, n_N is the nitrogen isotope atomic volumetric density, Γ is the nitrogen isotope diffusivity in water, R^N is the nitrogen isotope atomic volumetric density production rate and λ_N is the nitrogen isotope decay constant. This system is coupled with a nuclear problem as the source term, R^N , in the last equation, has a neutronic nature since it depends on the neutron flux which can be assessed by solving the neutron transport equation:

$$\begin{cases} R^N(\underline{x}) = \int_0^{+\infty} \int_{4\pi} \Sigma_{(n,p)}^{O-16/17}(\underline{x}, E) \varphi(\underline{x}, \underline{\Omega}, E) d\underline{\Omega} dE \\ \underline{\Omega} \cdot \nabla \varphi(\underline{x}, \underline{\Omega}, E) + \Sigma_t(\underline{x}, E) \varphi(\underline{x}, \underline{\Omega}, E) = \\ = \int_0^{+\infty} \int_{4\pi} \Sigma(\underline{\Omega}', E' \rightarrow \underline{\Omega}, E) \varphi(\underline{x}_i, \underline{\Omega}', E') d\underline{\Omega}' dE' + s(\underline{x}, \underline{\Omega}, E) \end{cases}$$

where: $\Sigma_{(n,p)}^{O-16/17}$ are the macroscopic cross sections of the reactions $^{16}\text{O}(n,p)^{16}\text{N}$ and $^{17}\text{O}(n,p)^{17}\text{N}$, φ is the angular neutron flux energy density, $\underline{\Omega}$ is the neutron direction unit vector, Σ_t is the total macroscopic cross section, Σ is the scattering kernel and s is the neutron source term. A steady state scenario has been taken into account for this coupled problem since the investigated

time domain is related to the plasma flat-top phase and because the nitrogen isotope concentrations, due to their short half-lives, reach saturation in an extremely small time compared to the duration of the aforementioned phase (2 hours).

The operative procedure adopted is based on a multi-physics method previously developed [12,13] and it foresees the assessment of the spatial distribution of nitrogen isotope concentration production rates within FW and BZ cooling channels and tubes by means of completely heterogeneous neutronic models of the Outboard Blanket (OB) and Inboard Blanket (IB) Breeder Unit Cells (BUCs). A fully 3-D CFD approach is, then, used to compute the nitrogen concentrations within the In-Vessel complex flow domain, while a lumped parameters, 1-D approach, is adopted to calculate the nitrogen isotope concentrations along the Ex-Vessel BB PHTS. Figure 1 represents the flow diagram of such a procedure.

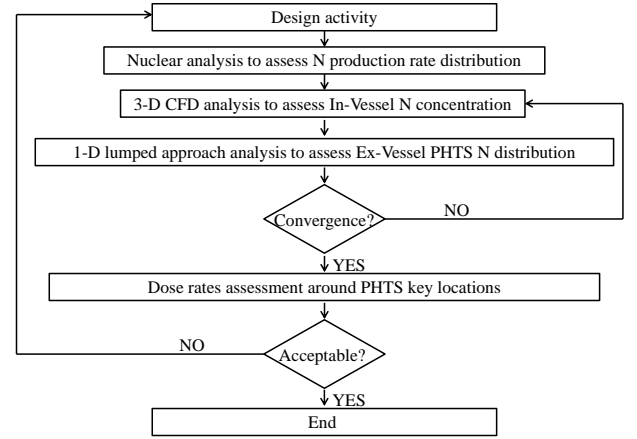


Fig. 1. Flow diagram of the coupling procedure set-up.

This flow diagram is characterized by two loops: the external one shows the feedback between this procedure and the design activity on the WCLL blanket while the inner one shows the iterative process to ensure the results from CFD analyses and lumped parameter ones match to one another. **It is to be further highlighted that the work shown in this paper doesn't concern the last part of the described procedure that is dose assessment.**

3. Assessment of the volumetric density of ^{16}N and ^{17}N production rates

The first step of the procedure described above foresees the assessment of the spatial distribution of ^{16}N and ^{17}N volumetric density production rates, therefore, neutronic analyses have been carried out for the cooling circuits of OB and IB FWs and for the OB BZ circuit while results have been extrapolated for the IB BZ circuit, which has not been considered as its design is not still mature enough. Neutronic analyses have been implemented adopting MCNP models representing toroidal – radial slices of the OB and IB [10] (Fig. 2). We focused the attention on equatorial BUCs and we extended the outcomes to the rest of the segments by scale factors taking into account both the poloidal profile of the Neutron Wall Load (NWL) [14] and the relative dimensions of the plasma facing surfaces.

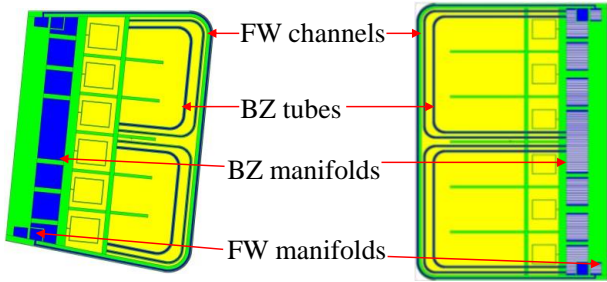


Fig. 2. Toroidal-radial sections of the IB (left) and OB (right) MCNP models of the WCLL BB slices.

It is to be highlighted that MCNP models are hybrid since the water domain is obtained by a UM geometry representation. In particular, ABAQUS C3D10 element type has been selected for all the models and every component has been set up, separately, in distinct ABAQUS parts. As far as boundary conditions are concerned, reflecting and white surfaces have been used in the poloidal and toroidal direction, respectively [12 – 13] to take into account the geometrical continuity in those directions. Regarding the neutron source

modelling, in DEMO reactor, neutrons enter the blanket directly from plasma or after scattering (albedo effect). In order to simulate such DEMO irradiation conditions, a local neutron source for the aforementioned WCLL BB slice models have been defined as a planar surface that emits neutrons biased in energies and cosines. More specifically, particle sampling in a DEMO global model (WCLL DEMO 2015 MCNP model) [15] allowed to evaluate the neutron emission probabilities in cosines and energies by tallying the surface neutron current across the plasma-facing surfaces of the slices taken into account in the global model. Figures 3 and 4 show the results obtained in terms of spatial distributions of ^{16}N and ^{17}N concentration production rates on FW cooling channels of both the OB and IB slices and on the OB BZ cooling tubes. Significant nitrogen production occurs only in the plasma-facing area of the channels and tubes, and then approaches quickly zero in the radial direction. These results are in line with the sharp radial gradient of neutron fast flux (not shown for sake of brevity), considering the high threshold energies of the involved nuclear reactions.

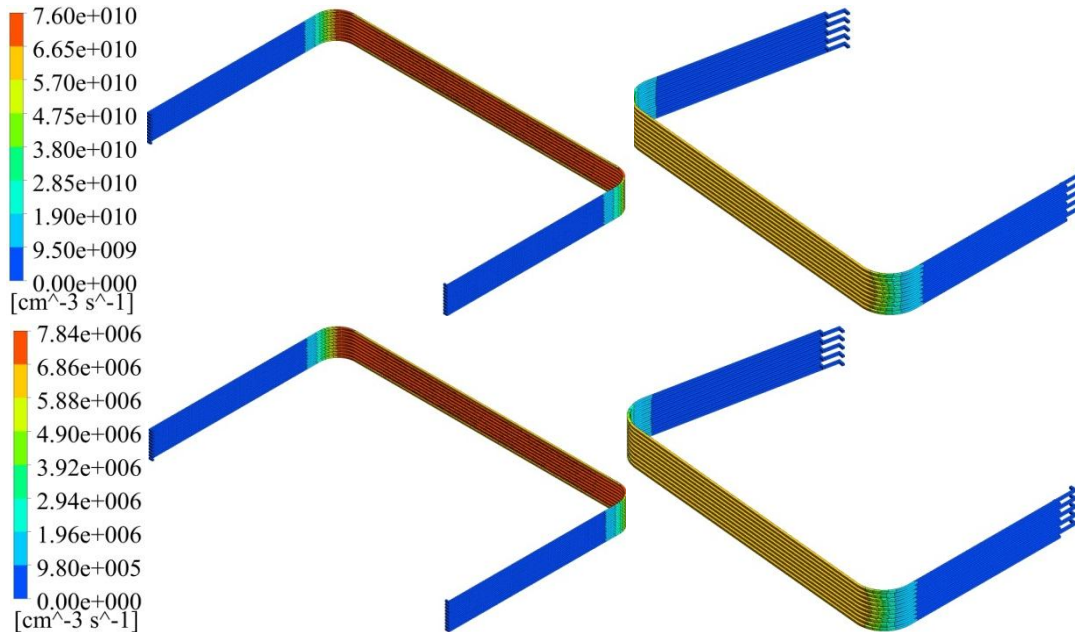


Fig. 3. Spatial distribution of ^{16}N and ^{17}N volumetric density production rates in the OB (left) and IB (right) FW.

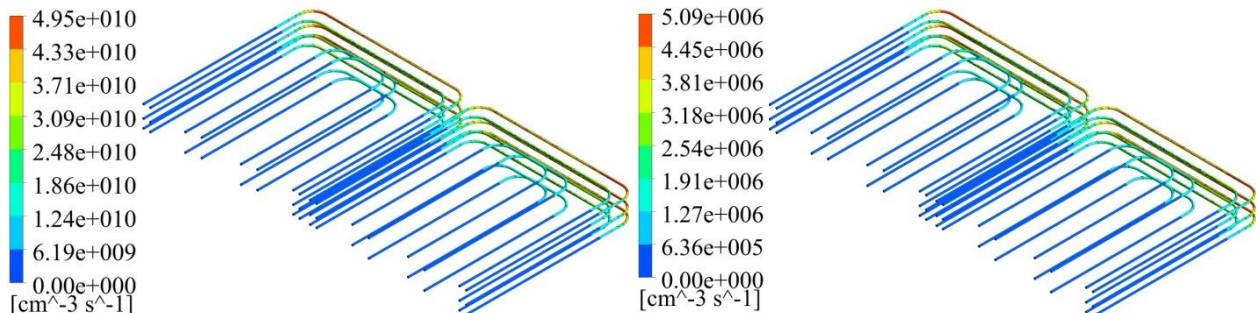


Fig. 4. Spatial distribution of ^{16}N (left) and ^{17}N (right) volumetric density production rates in the OB BZ.

4. Assessment of the volumetric densities of ^{16}N and ^{17}N in the FW and BZ hydraulic circuits

The second step of the procedure set-up considers the assessment of the spatial distribution of nitrogen isotopes concentrations in the in-Vessel side of the BB cooling

circuits by CFD analyses and in the ex-Vessel side by a 1-D approach.

4.1 Mass Flow rates evaluation

In order to determine such nitrogen isotope

concentration spatial distributions the knowledge of the mass flow rate in the cooling circuits under investigation is of uttermost importance, so, a dedicated CFD study has been carried out to assess the distribution of the mass flow rates in the FW channels of both the OB and IB segment, taking into account the total Balance of Plant (BoP) mass flow rate [9,10].

The assessment of mass flow rate distributions in the full FW OB and IB segments of the WCLL BB has been performed using porous media models for both the segments, for simulating each channel in which a hydraulic characteristic function is applied [7,16].

The central OB FW segment has been meshed with $3.61 \cdot 10^7$ nodes and $8.49 \cdot 10^7$ tetrahedral elements and the IB FW with $2.04 \cdot 10^7$ nodes, $4.75 \cdot 10^7$ tetrahedral elements, both the models have been simulated with a proper arrangement of the inflation layers which ensure a percentage of wetted surfaces close to 100% with a y^+ less than 100. The k- ϵ turbulent model has been adopted.

Figure 5 and 6 show the results for half the number of the channels for both the segments as they are two by two in countercurrent. The numeration of channels starts from the top to the bottom for OB FW and it follows the opposite direction for the IB FW. It can be noticed that these distributions are strongly asymmetric since they are not thermally optimized even though the total BoP mass flow rates have been used to evaluate them.

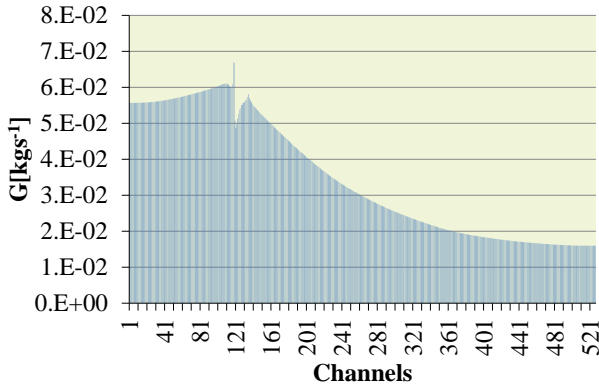


Fig. 5. Mass flow rate distribution in the OB FW channels.

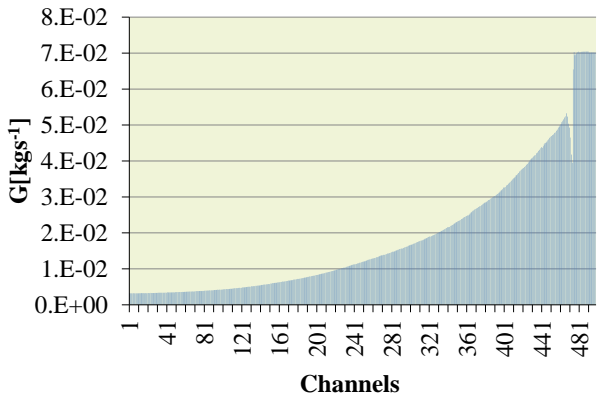


Fig. 6. Mass flow rate distribution in the IB FW channels.

Then, adopting a filter based on the NWL poloidal profile and on the percentage variation (10%) of mass flow rates among FW channels, 26 and 55 groups, that is

characteristic **BUCs**, have been selected as representative of the whole OB and IB segments respectively.

As regards the OB hydraulic circuits of the BZ, uniform flow rates have been considered for each channel, equal to the total BoP flow rate divided by the number of tubes per segment. As it will be explained later in this paper, this represents a conservative choice. Then, 7 regions (characteristic **BUCs**) have been selected as representative of the whole OB segment taking into account only the NWL poloidal profile.

4.2 Nitrogen isotope volumetric densities evaluation

The assessment of ^{16}N and ^{17}N volumetric densities in the FW channels of the 26 OB and 55 IB slices has been performed by CFD analyses.

As far as BZ tubes are concerned CFD analyses have been performed in one OB slice and results have been extrapolated to the whole segment scaling the values in accord to NWL neutron profile.

Nitrogen isotopes concentrations of the IB BZ water domain have been obtained from the OB BZ ones using scale factor taking into account both the ratios between the different NWL values and the mass flow rates related to the IB and OB segments.

Details about the water domain models set up are summarized in table 1.

Table 1. CFD FW mesh details.

| | OB FW | IB FW | OB BZ |
|----------------------------|--------------|--------------|--------------|
| Element Topology | Hexa | Hexa | Hexa |
| Nodes | 3054350 | 2286600 | 8243281 |
| Elements | 2904000 | 2173600 | 7966163 |
| Inflation layers number | 10 | 10 | 10 |
| First layer thickness [mm] | 4.81E-05 | 8.05E-05 | 4.81E-05 |
| Layers growth rate | 1.2 | 1.2 | 1.2 |
| Max. element size [m] | 2.00E-03 | 2.00E-03 | 2.00E-03 |
| Average element size [m] | 8.09E-04 | 8.09E-04 | 6.06E-04 |
| Surface with $y^+ < 60$ | 99.6% | 99.6% | 100.0% |

With regard to the boundary conditions adopted, the inlet mass flow rate and the outlet static pressure have been imposed for each channel and tube together with the following condition:

$$n_{N,Inlet} = n_{N,Outlet} e^{-\lambda \tilde{t}}$$

Where \tilde{t} represents the transit time of water in the hydraulic circuit outside the slices. From figures 7 and 8 which show the results obtained, it is possible to notice the effect of nitrogen isotopes transport within the flow domain, their maximum values being at the outlet sections of channels and tubes.

Moreover, the nitrogen concentrations have been evaluated at the outlet surface of every channel and tube to get the input data for the 1-D transport analyses related to the Ex Vessel components of the BB hydraulic circuits. As examples, in figures 9 and 10 are reported the ^{16}N volumetric densities at the outlet sections of the FW Channels of the OB and IB segments.

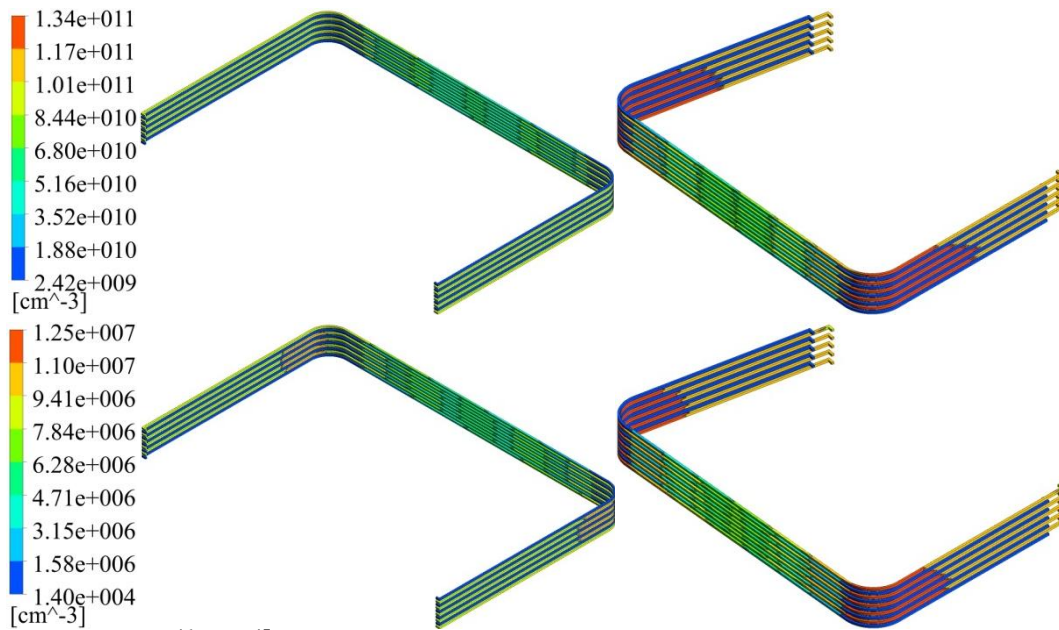


Fig. 7. Spatial distribution of ^{16}N and ^{17}N volumetric density in the OB (left) and IB (right) FW.

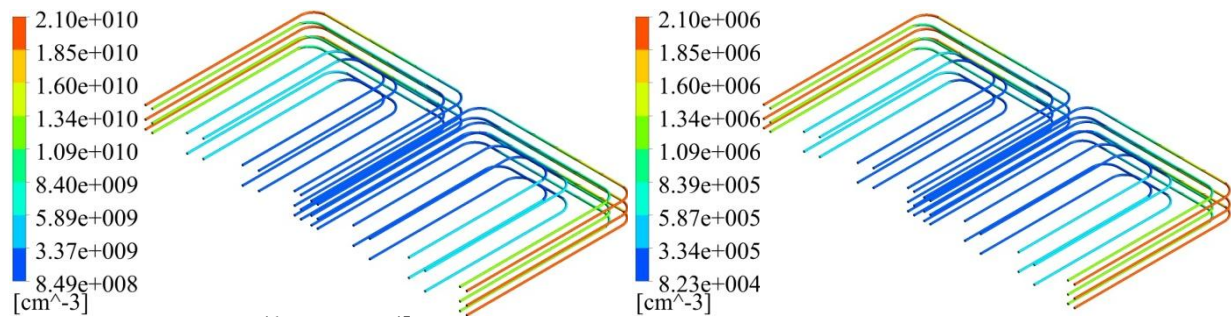


Fig. 8. Spatial distribution of ^{16}N (left) and ^{17}N (right) volumetric density in the OB BZ.

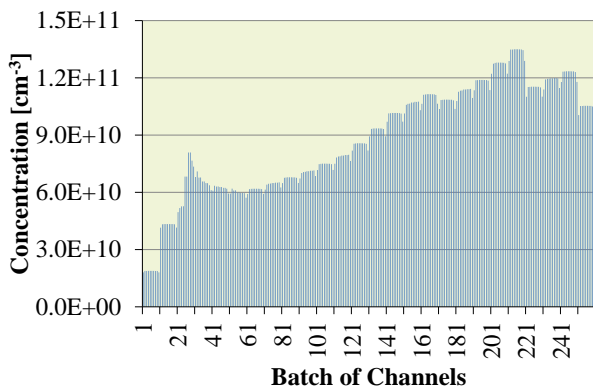


Fig. 9. ^{16}N concentration at the outlet of the OB FW channels.

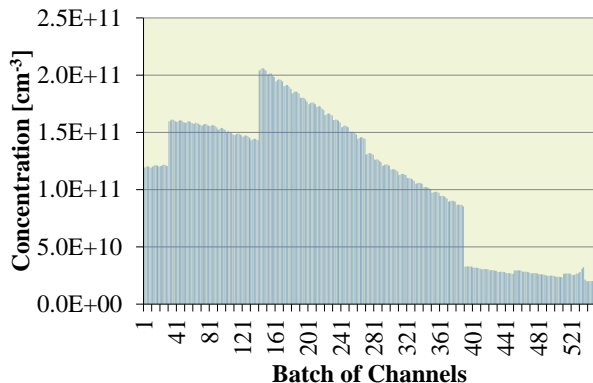


Fig. 10. ^{16}N concentration at the outlet of the IB FW channels.

4.3 1-D calculation results

As stated in the previous paragraphs, the assessment of ^{16}N and ^{17}N concentration spatial distributions in the Ex Vessel components has been carried out by a numerical method based on a 1-D lumped parameter approach that foresees a nodalization of the system.

As Nitrogen isotopes move from the single slice to the entire cooling system, it is necessary to account for the mixing of water streams in the collector pipes that transfer the coolant water to the PHTS (Figs. 11 and 12), modifying the nitrogen concentration distribution along the cooling system. So, it is necessary that the continuity equation is verified in each node of the system. Each slice, pipe and component of the cooling system is modelled as a node. Basically, for each node, it has been considered the balance between what enters from the previous nodes and what exits to the next nodes, decreased by the amount of nitrogen lost due to decay during the transit. The procedure is repeated for all the nodes in the system, and a new overall transit time is calculated. The application of this model allows to calculate a new and more precise transit time, so an iterative procedure has been performed to match results from the lumped calculations and CFD analyses. Few iterations have been proved sufficient in order to obtain accordance between the results.

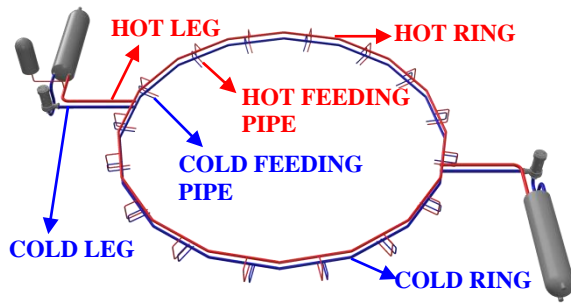


Fig. 11. Representation of the PHTS, FW hydraulic circuit.

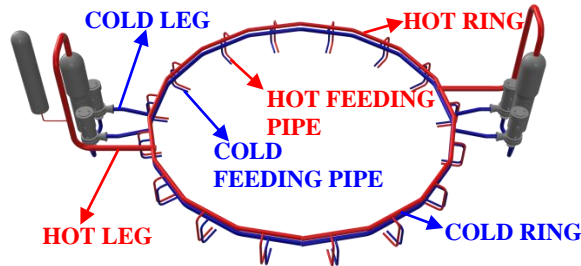


Fig. 12. Representation of the PHTS, BZ hydraulic circuit.

Table 2 and 3 show the results obtained in the most relevant components of the hydraulic circuits.

Table 2. Nitrogen concentration in the FW circuit [cm^{-3}].

| NODE | ^{16}N | ^{17}N |
|-------------------|-----------------|-----------------|
| Hot Feeding Pipe | 3.809E+10 | 2.338E+06 |
| Hot Ring | 3.031E+10 | 1.616E+06 |
| Hot Leg | 2.922E+10 | 1.518E+06 |
| Cold Leg | 5.248E+09 | 8.077E+04 |
| Cold Ring | 5.060E+09 | 7.589E+04 |
| Cold Feeding Pipe | 4.928E+09 | 7.257E+04 |

Table 3. Nitrogen concentration in the BZ circuit [cm^{-3}].

| NODE | ^{16}N | ^{17}N |
|-------------------|-----------------|-----------------|
| Hot Feeding Pipe | 4.516E+09 | 3.008E+05 |
| Hot Ring | 3.519E+09 | 2.012E+05 |
| Hot Leg | 2.578E+09 | 1.182E+05 |
| Cold Leg | 1.692E+09 | 5.758E+04 |
| Cold Ring | 1.627E+09 | 5.387E+04 |
| Cold Feeding Pipe | 1.577E+09 | 5.107E+04 |

In order to further investigate the effects of the distribution of the FW mass flow rates on isotopes transport, the assessment of the nitrogen isotopes concentrations in the PHTS has been carried out taking into account also uniform mass flow rates for both the OB and the IB, considering as reference values the ratios between the total OB and IB BoP flow rates and the number of channel per segment. In table 4 these results are shown under the label “Case 2” and compared with previous data related to not uniform FW flow rates (“Case 1”).

Table 4. Comparison between FW ^{16}N Concentrations [cm^{-3}].

| NODE | Case 1 | Case 2 | Δ [%] |
|-------------------|-----------|-----------|--------------|
| Hot Feeding Pipe | 3.809E+10 | 4.410E+10 | 15.78 |
| Hot Ring | 3.031E+10 | 3.509E+10 | 15.78 |
| Hot Leg | 2.922E+10 | 3.384E+10 | 15.85 |
| Cold Leg | 5.248E+09 | 6.080E+09 | 15.78 |
| Cold Ring | 5.060E+09 | 5.862E+09 | 15.85 |
| Cold Feeding Pipe | 4.928E+09 | 5.709E+09 | 15.78 |

It can be deduced how uniform flow rates imply higher nitrogen concentrations up to $\sim 16\%$, so that this

scenario can be assumed to be an extreme limit for this kind of problems. This occurrence will be useful in the WCLL BB design activity when real mass flow rates are available. Moreover, this result makes the results obtained rather conservative with reference to the calculations on the BZ hydraulic circuits.

5. Conclusion

Within the framework of EUROfusion action, at the University of Palermo a research campaign has been performed in order to assess the dose absorbed in some key components of the WCLL BB PHTS in the DEMO reactor. As first step of this research activity the main activation products of water (^{16}N and ^{17}N) volumetric densities have been evaluated in some relevant component of DEMO PHTS. To this purpose it has been developed a multi-physics method whose underlying idea is to evaluate the spatial distribution of nitrogen isotopes concentrations as precisely as possible in order to assess the spatial distribution of the absorbed dose in a realistic and accurate way. Therefore, the nitrogen isotopes production rates have been evaluated by neutronic analyses and their concentrations in the BB hydraulic circuits and in the PHTS system have been assessed by CFD analyses and 1-D lumped parameter calculations respectively. Then, results obtained have been used as input data to implement the neutronic and photonic sources necessary to assess the dose in the neighbourhood of the PHTS in a further work.

Acknowledgments

This work has been carried out within the framework of the EUROfusion Consortium and has received funding from the Euratom research and training programme 2014-2018 and 2019-2020 under grant agreement No 633053. The views and opinions expressed herein do not necessarily reflect those of the European Commission.

References

- [1] F. Cismondi et al., Progress of the conceptual design of the European DEMO Breeding Blanket, Tritium Extraction and Coolant Purification Systems. Presented at the 14th International Symposium On Fusion Nuclear Technology, Budapest, Hungary, 2019.
- [2] S. Jakhar, Nuclear Analysis of ^{16}N and ^{17}N radiation fields from TCWS activated water, ITER neutronics report, IDM reference ITER_D_QZ7BEK_v2.1, 2016.
- [3] N. Taylor, et al., ITER safety and licensing update, Fusion Eng. Des., 87 (2012) 476-481.
- [4] P. Chiovaro, et al., Assessment of the Dose Rates due to Water Activation on an Isolation Valve of the DEMO WCLL Breeding Blanket Primary Heat Transfer System. Presented at the 14th International Symposium On Fusion Nuclear Technology, Budapest, Hungary, 2019.
- [5] C.J. Werner, et al., MCNP6.2 Release Notes, Los Alamos National Laboratory, report LA-UR-18-20808 (2018).
- [6] JEFF3.2 Nuclear Data Library, (2018) http://www.oecd-nea.org/dbforms/data/eva/evatapes/jeff_32/.
- [7] Ansys Inc Ansys-Cfx Reference Guide, (2019), Release 19.2.

- [8] R. L. Martz, D. L. Crane, The MCNP6 Book On Unstructured Mesh Geometry: Foundations, LA-UR-12-25478v1 (2014).
- [9] L. Barucca, et al., Status of EU DEMO Heat Transport and Power Conversion Systems, Fusion Eng. Des., 136 (2018) 1557-1566.
- [10] A. Del Nevo, et al., Recent progress in developing a feasible and integrated conceptual design of the WCLL BB in EUROfusion project, Fusion Eng. Des. (2019), in press, DOI:10.1016/j.fusengdes.2019.03.040.
- [11] A. Tarallo, et al. Advancements in CAD implementation of EU-DEMO Water Cooled Lithium Lead Breeding Blanket primary heat transfer systems. Presented at the 14th International Symposium On Fusion Nuclear Technology, Budapest, Hungary, 2019.
- [12] Spagnuolo, G.A. et al., A multi-physics integrated approach to breeding blanket modelling and design, Fusion Eng. Des. (2018), in press, DOI: 10.1016/j.fusengdes.2019.03.131.
- [13] Favetti, R., et al., Validation of Multi-Physics Integrated Procedure for the HCPB Breeding Blanket, International Journal of Computational Methods (2019), in press, DOI: 10.1142/S0219876219500099.
- [14] F. Moro, et al., Neutronic analyses in support of the WCLL DEMO design development, Fusion Eng. Des., 136 (2018) 1260-1264.
- [15] P. Pereslvtsev, "2015 DEMO HCPB MCNP model", EUROfusion, IDM reference EFDA_2M5J2G, (2016).
- [16] R. Chen et al., Three dimensional thermal hydraulic characteristic analysis of reactor core based on porous media method, Annals of Nuclear Energy, vol. 104, pp. 178-190, 2017.